nature chemistry

ARTICLES

PUBLISHED ONLINE: 10 NOVEMBER 2014 | DOI: 10.1038/NCHEM.2108

Covalent functionalization of monolayered transition metal dichalcogenides by phase engineering

Damien Voiry[1], Anandarup Goswami[2,3], Rajesh Kappera[1], Cecilia de Carvalho Castro e Silva[1], Daniel Kaplan[4], Takeshi Fujita[5,6], Mingwei Chen[5], Tewodros Asefa[2,3] and Manish Chhowalla[1]*

Chemical functionalization of low-dimensional materials such as nanotubes, nanowires and graphene leads to profound changes in their properties and is essential for solubilizing them in common solvents. Covalent attachment of functional groups is generally achieved at defect sites, which facilitate electron transfer. Here, we describe a simple and general method for covalent functionalization of two-dimensional transition metal dichalcogenide nanosheets (MoS_2, WS_2 and $MoSe_2$), which does not rely on defect engineering. The functionalization reaction is instead facilitated by electron transfer between the electron-rich metallic 1T phase and an organohalide reactant, resulting in functional groups that are covalently attached to the chalcogen atoms of the transition metal dichalcogenide. The attachment of functional groups leads to dramatic changes in the optoelectronic properties of the material. For example, we show that it renders the metallic 1T phase semiconducting, and gives it strong and tunable photoluminescence and gate modulation in field-effect transistors.

Semiconducting single-layered transition metal dichalcogenides (TMDs) are interesting because they are direct-bandgap materials that have relatively good mobility values (up to ~100 $cm^2 V^{-1} s^{-1}$)[1]. Recent work has also demonstrated that they possess interesting catalytic properties for hydrogen evolution[2–5]. Chemical modification can further enhance the versatility of two-dimensional TMDs, for example, improving their solubility in common solvents. Ataca *et al.*[6] have theoretically investigated the functionalization of TMDs, but experimental reports of covalent functionalization remain scarce.

Nanosheets of TMDs can be obtained either by exfoliation (mechanical or chemical) of their bulk form, or by chemical vapour deposition[7]. Chemical exfoliation via butyllithium intercalation results in crystal phases with disparate electronic properties in the nanosheets[8,9]. For example, the trigonal prismatic semiconducting 2H phase is thermodynamically stable in MX_2 (where M = Mo or W and X = Se or S) TMDs from Group VI elements. However, butyllithium intercalation leads to partial conversion of the crystal structure from the 2H phase to the octahedral 1T metallic phase[8,10,11] due to electron transfer from the butyl group of the butyllithium to the TMD sheets (Fig. 1a,b).

Covalent functionalization of low-dimensional carbon-based materials at edges or defects present on the surface has been an active field of research over the past 20 years[12–14]. Several routes based on reactions of electrophiles with carbon atoms have also been reported[15–17]. In particular, functionalization has been achieved through reductive alkylation by adding a halide reagent to n-doped carbon nanotubes and graphene[15,18,19]. This approach has been extended recently to two-dimensional inorganic germanane nanosheets by Jiang and co-authors[20]. In contrast, current schemes for functionalization of TMDs consist of ligands interacting with unsaturated metal atoms at the edges or defects on the basal plane[21,22].

Results and discussion

Synthesis of functionalized TMD nanosheets. In this Article, we describe covalent functionalization of chemically exfoliated[25,26] MoS_2, WS_2 and $MoSe_2$ nanosheets containing a large fraction of 1T phase by reacting with organohalide solutions (2-iodoacetamide or iodomethane) (Supplementary Materials and Methods and Fig. 1a,b). Although we discuss the results from organohalide functionalized samples in the following, we have also carried out functionalization with aryl diazonium salts to demonstrate the versatility of our method. The diazonium salt functionalization results are described in Supplementary Section 'Functionalization with 4-bromobenzenediazonium tetrafluoroborate'. The functionalization reactions with 2-iodoacetamide or iodomethane were performed on uniformly dispersed 1T-phase single-layer nanosheets[3,10] (Supplementary Fig. 1). These reactions lead to functionalized TMD nanosheets, referred to as Fct-MX_2 (Fig. 1c). We also performed control experiments by treating the nanosheets in 0.15 M iodine in acetonitrile, a reaction in which charge is suppressed via mild oxidation and chemical functionalization is not induced (Fig. 1d)[23]. The products from these reactions were thoroughly washed with 2-propanol, ethanol and water, and were analysed with X-ray photoelectron spectroscopy (XPS). No signal from iodine was detected in the XPS survey spectra of functionalized and iodine-treated TMDs, indicating that unreacted starting reagents (2-iodoacetamide, iodomethane or iodine) were not present in the samples (Supplementary Fig. 3) after functionalization and control reactions. The zeta potential of functionalized nanosheet suspensions also increased significantly after the reaction due to suppression of excess charge and the attachment of functional groups (Supplementary Table 1). Chemically exfoliated nanosheets of TMDs containing a large

[1]Materials Science and Engineering, Rutgers University, 607 Taylor Road, Piscataway, New Jersey 08854, USA, [2]Department of Chemistry and Chemical Biology, Rutgers University, 610 Taylor Road, Piscataway, New Jersey 08854, USA, [3]Department of Chemical and Biochemical Engineering, Rutgers University, 98 Brett Road, Piscataway, New Jersey 08854, USA, [4]US Army RDECOM-ARDEC, Acoustics and Networked Sensors Division, Picatinny Arsenal, New Jersey 07806, USA, [5]WPI Advanced Institute for Materials Research, Tohoku University, Sendai 980-8577, Japan, [6]JST, PRESTO, 4-1-8 Honcho Kawaguchi, Saitama 332-0012, Japan. *e-mail: manish1@rci.rutgers.edu

© 2014 Macmillan Publishers Limited. All rights reserved.

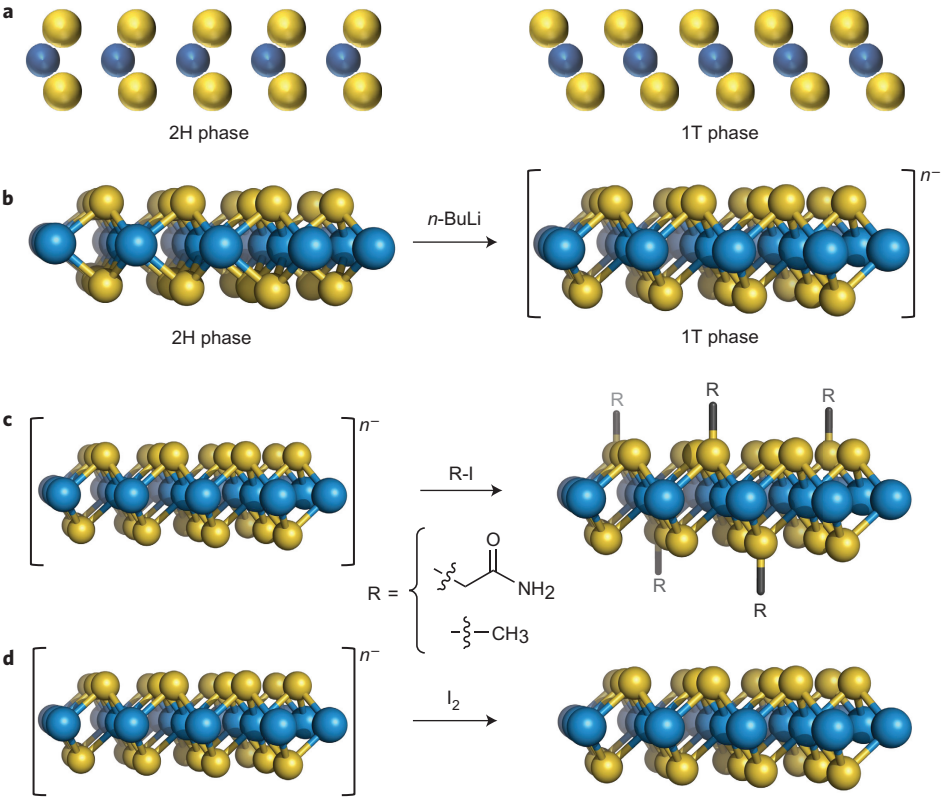

Figure 1 | Schematic of functionalization scheme. a, Side view of the 2H and 1T phases. **b**, The 2H phase of TMDs is converted to the 1T phase via lithiation using butyllithium (BuLi), and the 1T phase is negatively charged. n^- indicates the excess charges carried by the exfoliated 1T-phase nanosheets. **c**, The nanosheets are functionalized using 2-iodoacetamide or iodomethane (R-I) solution. **d**, The charge on the nanosheets can also be quenched by reacting with iodine, with no covalent functionalization.

fraction of 1T phase are charged, as indicated by zeta-potential measurements[23,24]. Heising and colleagues have estimated an excess charge of ~0.25 per MoS_2 nanosheet[23], which allows the nanosheets to remain in suspension. The 2H phase of the TMDs is not charged and 2H nanosheets cannot therefore be stabilized in common solvents.

Characterization. Chemically exfoliated nanosheets contain a mixture of 1T and 2H phases. The phase concentration and degree of functionalization were estimated by XPS. The 1T-phase concentrations were found to be ~65%, ~75% and ~65% for MoS_2, WS_2 and $MoSe_2$, respectively. Functionalization of the TMD nanosheets after reaction with 2-iodoacetamide was confirmed by observing signals from N1*s* and C1*s* regions in XPS at ~400 eV and ~288.4 eV, respectively (Fig. 2 and Supplementary Fig. 4). XPS analyses also revealed that the 1T- and 2H-phase concentrations are preserved after the functionalization reaction. We have estimated the degree of functionalization by calculating the ratio of the amount of nitrogen (from the amide) to metal atoms. According to XPS, the ratio of functional groups per MX_2 reaches 29 at%, 25 at% and 32 at% for Fct-MoS_2, Fct-WS_2 and Fct-$MoSe_2$, respectively. If the excess charge on the nanosheets is ~25%, as reported by Heising[23], then these concentrations suggest that our functionalization reactions are highly efficient. Furthermore, the XPS analyses did not reveal the formation of MO_x (M = Mo or W) or XO_x (X = S or Se) (Fig. 2 and Supplementary Fig. 5). It can be seen in Fig. 2 (right-hand spectra) that the S2*p* (panels a,b) and Se3*d* (panel c) peaks become slightly more pronounced relative to the spectra from reference samples after functionalization, suggesting that attachment of the functional group occurs on the S or Se (Fig. 2). Thermogravimetric analysis (TGA) revealed that the degree of functionalization (measured from weight losses) was 20 at %, 19 at% and 25 at% for Fct-MoS_2, Fct-WS_2 and Fct-$MoSe_2$, respectively, in reasonably good agreement with the XPS results (Supplementary Fig. 6).

Attenuated total reflectance Fourier transform infrared (ATR-FTIR) spectroscopy was used to confirm covalent functionalization of the TMD nanosheets. For ATR-FTIR we used iodomethane to functionalize the nanosheets with methyl groups because of their higher infrared sensitivity. The resulting spectra are less complicated, so the peaks can be clearly identified (Supplementary Methods). The ATR-FTIR spectra of the methyl-functionalized TMD nanosheets are shown in Fig. 3. It can be seen that the methyl-functionalized MoS_2 displays strong signals at 1,295 cm^{-1} and 943 cm^{-1}, which are attributed to the methyl deformation and rocking modes, respectively, originating from S–CH_3. No signal from unreacted iodomethane was detected. The S–C stretching at 700 cm^{-1} (refs 27,28) is also clearly observed. Similar signatures are also seen for WS_2, with peaks at 1,293 cm^{-1} and 947 cm^{-1} for the -CH_3 bands and 811 cm^{-1} and 700 cm^{-1} for the S–C bands. Interestingly, similar peaks are down-shifted by ~50 cm^{-1} in the case of $MoSe_2$. Methyl deformation and rocking modes are found at 1,246 cm^{-1} and 890 cm^{-1}, respectively, whereas Se–C stretching is visible at 605 cm^{-1} (refs 27–29). ATR-FTIR analysis strongly suggests that the attachment of the functional groups is located on the chalcogen atoms. Raman spectroscopy provides additional evidence of covalent functionalization with a split of the out-of-plane A_{1G} mode, most probably due to the presence of functional groups attached to the chalcogen atoms (Supplementary Fig. 9).

To further elucidate the location of functionalization sites on the TMD nanosheets, we performed solid-state ^{13}C CP-MAS NMR (cross-polarization magic angle spinning NMR) spectroscopy on

© 2014 Macmillan Publishers Limited. All rights reserved.

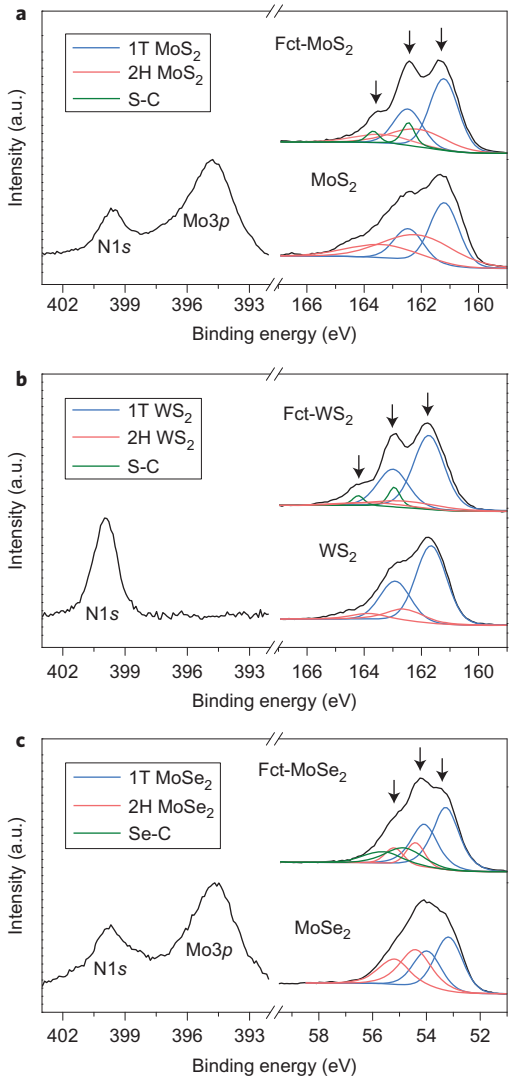

Figure 2 | XPS spectra of functionalized TMDs. a–c, High-resolution spectra from the N1*s* and Mo3*p* (left-hand spectra), and either S2*p* or Se3*d* (right-hand spectra) regions from MoS_2 (**a**), WS_2 (**b**) and $MoSe_2$ (**c**). Chemically exfoliated TMDs contain a mixture of 1T and 2H phases. The XPS peak of the 1T phase is downshifted by ~0.9 eV relative to the 2H peak[10]. The overall signal for each TMD material is shown in black, signals from the C–S/Se bond, 1T and 2H phases are shown in green, blue and red, respectively. The presence of the N1*s* signal at ~400 eV for acetamide-functionalized TMDs confirms attachment of the amide functional groups on the surface of the nanosheets. Peaks associated with the 1T phase, S–C and Se–C components become more pronounced after functionalization, as indicated by arrows.

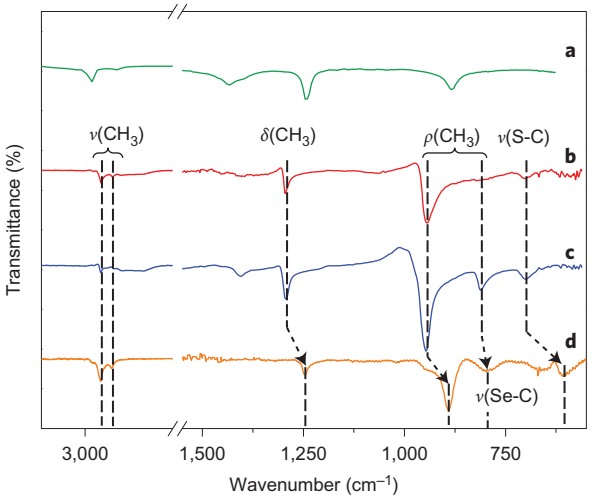

Figure 3 | ATR-FTIR spectra of methyl-functionalized TMDs. a–d, Spectra of iodomethane (green, **a**), functionalized 1T MoS_2 (red, **b**), functionalized 1T WS_2 (blue, **c**) and functionalized 1T $MoSe_2$ (orange, **d**) showing stretching (ν) deformation (δ) and rocking (ρ) modes. The -CH_3 and Se–C vibration modes are notably shifted for $MoSe_2$ compared with modes for MoS_2 and WS_2, indicating that covalent attachment of functional groups occurs via the chalcogen atoms.

the acetamide-functionalized nanosheets (Fig. 4). Because of the intrinsic parameter settings of the ^{13}C CP-MAS experiment, only qualitative data were obtained regarding the different chemical environments experienced by the different classes of carbon atoms in the material(s). The spectra were referenced with an external adamantane standard in which the peak at higher chemical shift was set at 38.43 ppm. As shown in Fig. 4a, 2-iodoacetamide shows characteristic chemical shifts (δ) corresponding to carbonyl and aliphatic carbons (α-C in this case) at 178.3 ppm and 4.6 ppm (shown in green and blue, respectively). This spectrum, when compared to the acetamide spectrum (Supplementary Fig. 10), showed a significant difference in the aliphatic region due to the difference in the electronic environments of the α-C. As well as the difference in chemical shifts, the broadness for 2-iodoacetamide can also be associated with the heteroatom (in this case iodine) connected to α-C. In the case of Fct-MoS_2 (Fig. 4b), peaks corresponding to both α-C and carbonyl were shifted from those of the 2-iodoacetamide precursor. The downfield shift of α-C (δ 49.6 ppm) compared to 2-iodoacetamide clearly indicates the presence of a different carbon-heteroatom linkage, stemming from covalent functionalization. Although the slight difference in chemical shift values of Fct-MoS_2 and Fct-WS_2 (Fig. 4d) indicates different functionalized materials, it also reveals that, despite having two different metals, it is the primary point of attachment (in this case S, as evident from XPS results) on the surface that dictates the chemical shifts. This effect becomes prominent when S (as the primary point of attachment) is replaced by Se (as in the case of Fct-$MoSe_2$, Fig. 4e). In that case, the chemical shift corresponding to the α-C moved significantly to an up-field value (δ 35.2 ppm) compared to either Fct-MoS_2 or Fct-WS_2. The high degree of functionalization (>20 at%) combined with evidence of C–S or C–Se bonding indicates that the attachment occurs mostly at the surface of the nanosheets and not at the edges or defects alone.

Additional control experiments were performed to confirm that functionalization is not mediated by defects. First, we replaced TMD nanosheets containing the electron-rich 1T phase with nanosheets containing only the 2H phase. According to XPS spectroscopy, no N1*s* peak from the amide group was detected on the 2H-phase TMD nanosheets. We also mixed acetamide only with the 1T phase of TMDs, and again no reaction was observed according to XPS, confirming the role of the iodide (most likely as a leaving group) in the grafting reaction (Supplementary Fig. 12).

Optical properties. For this phase of the study we used electronic-grade single-layer 2H MoS_2 nanosheets grown by chemical vapour deposition (CVD) (see Supplementary Section 'Materials and methods' for growth conditions). It can be seen from Fig. 5a that the CVD nanosheets are highly photoluminescent[30,31], with a photoluminescence energy of ~1.8 eV, consistent with a direct-bandgap transition at the K-point in the band structure of monolayered 2H MoS_2 (ref. 31). In contrast, when the same

© 2014 Macmillan Publishers Limited. All rights reserved.

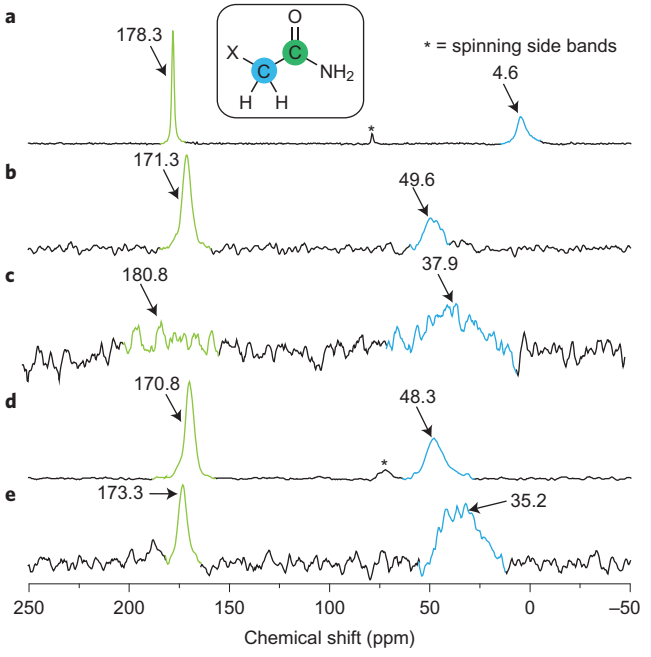

Figure 4 | NMR spectra for functionalized TMDs. a–e,^{13}C CP-MAS spectra of 2-iodoacetamide (**a**) and functionalized 1T MoS_2 (**b**), 300 °C-annealed functionalized MoS_2 (**c**), functionalized 1T WS_2 (**d**) and functionalized 1T $MoSe_2$ (**e**). Green peaks designate the C signals corresponding to carbonyls and blue peaks show α-C signals. The peaks arising from the α-C (blue) are shifted relative to free iodoacetamide, whereas the carbonyl C (green) peaks remain relatively constant. The fact that the α-C peaks remain relatively constant in curves **b** and **d** suggests that bonding is through the sulfur atoms in MoS_2 and WS_2.

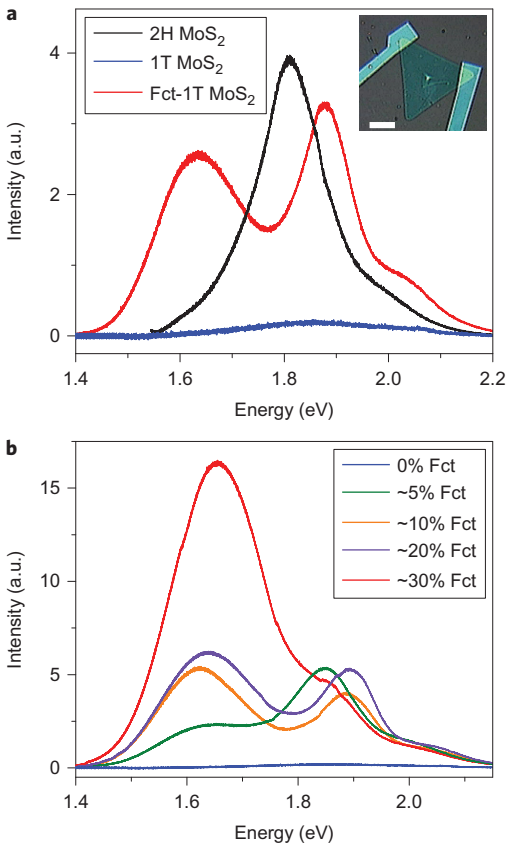

Figure 5 | Photoluminescence from functionalized 1T-phase MoS_2. **a**, Photoluminescence spectra obtained from single-layer MoS_2 grown by CVD (2H phase), from the metallic 1T phase and from the functionalized 1T phase. A strong photoluminescence peak at ~1.8 eV is observed for the 2H phase, consistent with single-layer 2H MoS_2, whereas photoluminescence is quenched after conversion to the metallic 1T phase. The functionalized 1T phase exhibits strong photoluminescence, characterized by two bands at ~1.9 eV and ~1.6 eV. Inset: a typical CVD-grown monolayer triangular nanosheet on which the photoluminescence spectra were measured. Scale bar, 25 μm. **b**, Modulation of photoluminescence peak intensity with increasing amount of functionalization: blue, 0% Fct; green, ~5% Fct; orange, ~10% Fct; purple, ~20% Fct; red, ~30% Fct. Photoluminescence peaks are normalized to the Raman peak of silicon at 520 cm^{-1}.

monolayered CVD MoS_2 is converted to the 1T phase via butyllithium treatment (see Methods), photoluminescence is completely suppressed[10]. Interestingly, intense photoluminescence reappears after functionalization of the monolayered 1T-phase CVD nanosheet. The photoluminescence in the functionalized 1T-phase sample consists of two primary peaks: one at ~1.9 eV, which is the shifted MoS_2 peak, and the other at ~1.6 eV, which may be attributed to band-structure modification due to covalent functionalization. Recently, such a peak has been correlated to bound excitons resulting from defects in monolayer TMDs[32]. This is supported by the fact that the intensity of the 1.6 eV photoluminescence peak can be tuned by varying the concentration of the functional groups on the nanosheets, as shown in Fig. 5b. We also confirmed the metallic to semiconducting conversion of the 1T phase after functionalization by measuring the field-effect transistor (FET) properties of the functionalized 1T phase (see Supplementary Section 'Field effect transistors' for details).

Functionalization of the 2H phase. We have shown above that the 2H phase cannot be functionalized directly. It is, however, possible to functionalize the 1T phase and relax it to the functionalized 2H phase through annealing. Functionalized 1T-phase MoS_2 was annealed up to 300 °C to progressively restore the 2H phase (Supplementary Materials and Methods). Upon annealing at 300 °C, Fct-MoS_2 transforms to 100% semiconducting 2H phase (Supplementary Figs 14–17). ^{13}C CP-MAS NMR results also suggest the presence of functional groups on the 2H MoS_2 nanosheets, albeit with a large decrease in the signal-to-noise ratio (Fig. 4c). A similar amount of functionalization was obtained for 2H WS_2 (Supplementary Fig. 14). Signatures of the S–CH_3 and S–C bonds can also be clearly identified in the ATR-FTIR spectra of the functionalized 2H phase (Supplementary Fig. 13).

Conclusions

We have reported a general scheme for covalent functionalization of TMDs. The reaction, based on the addition of amide and methyl moieties (from organoiodide precursors), was successfully applied to sulfur- and selenium-based TMDs. Functional groups were grafted directly onto the chalcogen layer of nanosheet surfaces. The extent of functionalization was up to 30 at% relative to the transition metal content, equivalent to a density of ~3×10^{14} molecules cm^{-2} on the basal plane. After functionalization, the properties of the 1T phase are profoundly altered from metallic to semiconducting, giving rise to strong and tunable photoluminescence. The anchoring of functional groups on the nanosheets should open new routes for further chemical modification of TMD nanosheets.

Methods

TMD exfoliation. Caution: n-butyllithium is highly pyrophoric. MoS_2, WS_2 and $MoSe_2$ were exfoliated following the method reported in refs 3 and 10. Briefly, bulk powder of TMDs (0.3 g) was mixed with n-butyllithium (3 ml, 1.6 M in hexane) and heated at reflux under argon for 48 h. The mixture was then filtered under argon and washed with hexane to remove excess butyllithium. The intercalated powder was exfoliated in water at 1 mg ml^{-1}, sonicated for 1 h to facilitate the exfoliation, and centrifuged to remove lithium compounds as well as the non-exfoliated materials.

© 2014 Macmillan Publishers Limited. All rights reserved.

Iodine treatment of exfoliated TMDs. Typically, 15 mg exfoliated TMDs was transferred into acetonitrile. The nanosheets were treated with 15 ml of 0.15 M iodine solution in acetonitrile. After 5 days of reaction at room temperature TMDs were washed thoroughly with acetonitrile (6 × 50 ml), 2-propanol (3 × 50 ml), ethanol (3 × 50 ml) and water (3 × 50 ml).

Functionalization of TMDs. 2-Iodoacetamide was added to the water solution of exfoliated TMDs with tenfold excess. After 5 days of reaction at room temperature, the materials were washed with 2-propanol (3 × 50 ml), ethanol (3 × 50 ml) and water (3 × 50 ml).

Functionalization of single-layer MoS_2 nanosheets grown by CVD. Single-layer MoS_2 flakes grown by CVD on SiO_2 were first converted to the 1T phase. In a glove box, butyllithium (1.6 M in hexane) was dropped on the wafer. After 24 h of reaction, the wafer was washed with hexane (4 × 2 ml) and dried. 0.1 M of 2-iodoacetamide in dimethylsulfoxide was then added to the MoS_2 flakes and the reaction was carried out for 48 h. Finally, excess 2-iodoacetamide solution was removed and the wafer was washed with dimethylsulfoxide (DMSO, 2 × 5 ml), THF (2 × 5 ml), 2-propanol (2 × 5 ml), ethanol (2 × 5 ml) and water (2 × 5 ml).

XPS measurements were performed with a Thermo Scientific K-Alpha spectrometer with a detection limit of 0.1 at%. All spectra were taken using a Al-Kα microfocused monochromatized source (1,486.6 eV) with a resolution of 0.6 eV and a spot size of 400 μm. Photoluminescence spectra were obtained using a Renishaw 1000 system operating at 514 nm (2.41 eV).

ATR FTIR spectra were obtained on a PerkinElmer Spectrum One FTIR spectrometer equipped with a universal diamond ATR reflection top-plate. Spectra were collected by pressing the sample onto a diamond crystal with a pressure setting of 90 on the DuraScope. Each spectrum consisted of 16 spectra co-added accumulated between 4,000 cm^{-1} and 560 cm^{-1} with a spectral resolution of 4 cm^{-1}. Iodine-treated TMDs were used as background.

The solid-state ^{13}C (100.64 MHz) NMR spectra were acquired on a Bruker 400 MHz NMR spectrometer (with a Bruker 3.2 mm bore HXY probe operating in HX mode) at 298 K. The samples were prepared mixing cal-SBA-15 with the samples followed by careful packing of the mixture into a 3.2 mm zirconia rotor. For ^{13}C CP-MAS NMR experiments, a 10.0 kHz spin rate, 5 s recycle delay, 2 ms contact time, π/2 pulse width of 5 μs (at 66 W) and at least 64 K scans using 'Spinal 64' ^{1}H decoupling method were used. The spectra were referenced based on an external adamatane standard in which the peak at higher chemical shift was set at 38.43 ppm. The spectra were processed in a Bruker Topspin (*v* 3.2) using conventional techniques, and a 50 Hz line broadening window function was applied to all spectra.

Received 11 May 2014; accepted 7 October 2014; published online 10 November 2014

References

1. Wang, Q. H., Kalantar-Zadeh, K., Kis, A., Coleman, J. N. & Strano, M. S. Electronics and optoelectronics of two-dimensional transition metal dichalcogenides. *Nature Nanotech.* **7,** 699–712 (2012).
2. Jaramillo, T. F. *et al.* Identification of active edge sites for electrochemical H_2 evolution from MoS_2 nanocatalysts. *Science* **317,** 100–102 (2007).
3. Voiry, D. *et al.* Enhanced catalytic activity in strained chemically exfoliated WS_2 nanosheets for hydrogen evolution. *Nature Mater.* **12,** 850–855 (2013).
4. Lukowski, M. A. *et al.* Enhanced hydrogen evolution catalysis from chemically exfoliated metallic MoS_2 nanosheets. *J. Am. Chem. Soc.* **135,** 10274–10277 (2013).
5. Voiry, D. *et al.* Conducting MoS_2 nanosheets as catalysts for hydrogen evolution reaction. *Nano Lett.* **13,** 6222–6227 (2013).
6. Ataca, C. & Ciraci, S. Functionalization of single-layer MoS_2 honeycomb structures. *J. Phys. Chem. C* **115,** 13303–13311 (2011).
7. Chhowalla, M. *et al.* The chemistry of two-dimensional layered transition metal dichalcogenide nanosheets. *Nature Chem.* **5,** 263–275 (2013).
8. Py, M. A. & Haering, R. R. Structural destabilization induced by lithium intercalation in MoS_2 and related compounds. *Can. J. Phys.* **61,** 76–84 (1983).
9. Heising, J. & Kanatzidis, M. G. Structure of restacked MoS_2 and WS_2 elucidated by electron crystallography. *J. Am. Chem. Soc.* **121,** 638–643 (1999).
10. Eda, G. *et al.* Photoluminescence from chemically exfoliated MoS_2. *Nano Lett.* **11,** 5111–5116 (2011).
11. Eda, G. *et al.* Coherent atomic and electronic heterostructures of single-layer MoS_2. *ACS Nano* **6,** 7311–7317 (2012).
12. Tasis, D., Tagmatarchis, N., Bianco, A. & Prato, M. Chemistry of carbon nanotubes. *Chem. Rev.* **106,** 1105–1136 (2006).
13. Hirsch, A. Functionalization of single-walled carbon nanotubes. *Angew. Chem. Int. Ed.* **41,** 1853–1859 (2002).
14. Quintana, M., Vazquez, E. & Prato, M. Organic functionalization of graphene in dispersions. *Acc. Chem. Res.* **46,** 138–148 (2013).
15. Liang, F. *et al.* A convenient route to functionalized carbon nanotubes. *Nano Lett.* **4,** 1257–1260 (2004).
16. Voiry, D., Roubeau, O. & Pénicaud, A. Stoichiometric control of single walled carbon nanotubes functionalization. *J. Mater. Chem.* **20,** 4385–4391 (2010).
17. Syrgiannis, Z. *et al.* Reductive retrofunctionalization of single-walled carbon nanotubes. *Angew. Chem. Int. Ed.* **49,** 3322–3325 (2010).
18. Chakraborty, S., Chattopadhyay, J., Guo, W. & Billups, W. E. Functionalization of potassium graphite. *Angew. Chem. Int. Ed.* **46,** 4486–4488 (2007).
19. Englert, J. M. *et al.* Covalent bulk functionalization of graphene. *Nature Chem.* **3,** 279–286 (2011).
20. Jiang, S. *et al.* Improving the stability and optical properties of germanane via one-step covalent methyl-termination. *Nature Commun.* **5,** 3389 (2014)
21. Canfield, D. & Parkinson, B. A. Improvement of energy conversion efficiency by specific chemical treatments of molybdenum selenide (n-$MoSe_2$) and tungsten selenide (n-WSe_2) photoanodes. *J. Am. Chem. Soc.* **103,** 1279–1281 (1981).
22. Chou, S. S. *et al.* Ligand conjugation of chemically exfoliated MoS_2. *J. Am. Chem. Soc.* **135,** 4584–4587 (2013).
23. Heising, J. & Kanatzidis, M. G. Exfoliated and restacked MoS_2 and WS_2: ionic or neutral species? Encapsulation and ordering of hard electropositive cations. *J. Am. Chem. Soc.* **121,** 11720–11732 (1999).
24. Golub, A. S., Zubavichus, Y. V., Slovokhotov, Y. L., Novikov, Y. N. & Danot, M. Layered compounds assembled from molybdenum disulfide single-layers and alkylammonium cations. *Solid State Ion.* **128,** 151–160 (2000).
25. Joensen, P., Frindt, R. F. & Morrison, S. R. Single-layer MoS_2. *Mater. Res. Bull.* **21,** 457–461 (1986).
26. Yang, D. & Frindt, R. F. Li-intercalation and exfoliation of WS_2. *J. Phys. Chem. Solids* **57,** 1113–1116 (1996).
27. Socrates, G. *Infrared and Raman Characteristic Group Frequencies: Tables and Charts* (Wiley, 2001).
28. Aynsley, E. E., Greenwood, N. N. & Sprague, M. J. The oxidation of potassium selenocyanate by iodine pentafluoride. *J. Chem. Soc. (Resumed)* 704–708 (1964).
29. Khan, M. A. & Raees, H. ChemInform abstract: synthesis of a new bis-harmine selenide. *ChemInform* **28,** 1779–1780 (1997).
30. Mak, K. F., Lee, C., Hone, J., Shan, J. & Heinz, T. F. Atomically thin MoS_2: a new direct-gap semiconductor. *Phys. Rev. Lett.* **105,** 136805 (2010).
31. Splendiani, A. *et al.* Emerging photoluminescence in monolayer MoS_2. *Nano Lett.* **10,** 1271–1275 (2010).
32. Tongay, S. *et al.* Defects activated photoluminescence in two-dimensional semiconductors: interplay between bound, charged, and free excitons. *Sci. Rep.* **3,** 2657 (2013).

Acknowledgements

M. Chhowalla, D.V. and R.K. acknowledge financial support from the National Science Foundation Division of Graduate Education (NSF DGE) 0903661. T.A. and A.G. acknowledge financial assistance from the NSF (CAREER Chemistry-1004218, DMR-0968937, NanoEHS-1134289, NSF-Analytical Chemistry Instrumentation Facility and a Special Creativity Grant). C.S. acknowledges the Conselho Nacional de Desenvolvimento Científico e Tecnológico-Brazil, for a fellowship. T.F. acknowledges partial support from Japan Science and Technology Agency-PRESTO ('New Materials Science and Element Strategy') and Japan Society for Promotion of Science (Grant-in-Aid for Scientific Research on Innovative Areas 'Science of Atomic Layers', 90363382). The authors thank G.S. Hall for ATR-FTIR measurements. G. Recine at New York University Polytechnic is thanked for computing time.

Author contributions

M. Chhowalla conceived the idea and designed the experiments. D.V. conceived the idea and designed the experiments with M. Chhowalla, functionalized the TMDs, characterized them with Raman, TGA, UV-vis and XPS analysis. M. Chhowalla and D.V. analysed the data and wrote the manuscript. R.K. fabricated the field-effect transistors and helped C.S. with FET measurements. C.S. measured FET performance. D.K. performed first-principles calculations of the atomic structure of functionalized MoS_2. T.F. and M. Chen performed the STEM work. A.G. carried out the ^{13}C NMR, XRD and FTIR experiments. A.G. and T.A. discussed the results with M. Chhowalla and D.V.

Additional information

Supplementary information is available in the online version of the paper. Reprints and permissions information is available online at www.nature.com/reprints. Correspondence and requests for materials should be addressed to M. Chhowalla.

Competing financial interests

The authors declare no competing financial interests.

© 2014 Macmillan Publishers Limited. All rights reserved.